Al-Azhar University Civil Engineering Research Magazine (CERM)
Vol. (41) No. (2) April, 2019

Effect of Concrete Strength and Depth on the behavior of Simple R.C Deep Beams using finite element analysis

Ayman Hussein Khalil[1], Mahmoud Mohamed El-Kateb[2], and Shaimaa Mostafa Ahmed[3]

1 Professor of Reinforced Concrete Structures, 2 Assistant Professor of Reinforced Concrete Structures, and 3 structural Engineer at Q Design

Structural Department, Ain Shams University, Cairo, Egypt

ملخص البحث:

تم فى هذا البحث عرض وتحليل النتائج لمجموعة من الكمرات الخرسانية المسلحة العميقة بسيطة الارتكاز ذات حمل مركز فى منتصف البحر وذلك باستخدام برنامج العناصر المحددة(ANSYS 16.0) وكذلك تأثير كل من مقاومة الضغط للخرسانة والعمق على مقاومة القص للكمرات.المتغيرات التى تم دراستها هى النسبة بين مسافة القص الى العمق(a/t) ونسبة حديد القص الرأسى (ρ_{vL})والقص الافقى (ρ_{HZ}) والحديد الطولى العلوى والسفلى (ρ_L)وقد أظهرت تلك الدراسة انخفاض فى قيم مقاومة القص عند زيادة قيمة (a/t).

Abstract

This paper presents an analytical study of sixteen reinforced concrete simple deep beams with a concentrated load using finite element analysis (ANSYS 16.0 software). This paper also studies the influence of cube compressive strength of concrete, percentage of longitudinal steel, and the effect of depth on the behavior and failure load of concrete deep beams, the parameters considered are percentage of longitudinal steel which varied from 0.40 to 2%, shear span to depth ratio (a/t) are varied from 2 to 1, and cube compressive strength of concrete which varied from 40MPa to 100MPa.The results of the study give a prediction for the shear strength.

1. Introduction

Deep beams are structural elements with relatively large depth used as load distribution carrying elements such as (transfer girders, pile caps, tank walls, and retaining walls) often receiving many small loads and transferring them to reaction points.

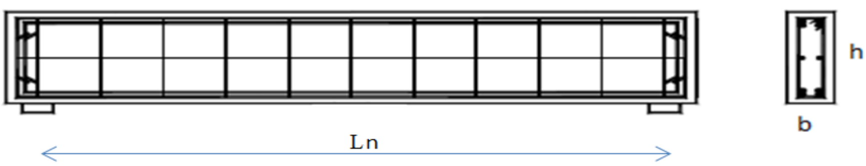

Figure (1) Geometry of Simple Deep Beam

According to (ECP 203-2007) [1], Deep beams are characterized as beams whose effective span to depth ratios greater than 1.25 for the simple beams and 2.50 for the continuous beams. According to (ACI Committee 318, 2008)[2] Deep beams are members that are loaded on one face and supported on the opposite face such that strut-like compression elements can develop between the loads and supports and that satisfy A or B

- **A.** Clear span doesn't exceed four times the overall member depth (h).
- **B.** Concentrated loads exist within a distance (2h) from the face of the support.

Due to the small value of the span-to-depth ratio, the failure of deep beams is controlled by shear rather than flexure. The basic assumption of the plane section assumed to remain plane after bending is not valid for deep beams. It has a nonlinear stress distribution along the depth of the beam. The shear strength of concrete deep beams can be predicted by the models proposed by existing codes of practices namely, IS 456(2000) [3], ACI 318 (2008)

[2], JSCE (2007) [4], CSA(2004)[5], BS 8110[6] and by the models proposed by various researchers, namely, Zsutty (1968)[7], Mau and Hsu(1989)[8], Matamoros and Wong (2000)[9], and Park and Kuchma (2007)[10] etc. The shear strength of concrete beams can also be predicted by numerical methods. In this paper, a concrete deep beam subjected to three points loading has been considered. The shear strength is predicted using the numerical model proposed by ANSYS 16.0[11] software.

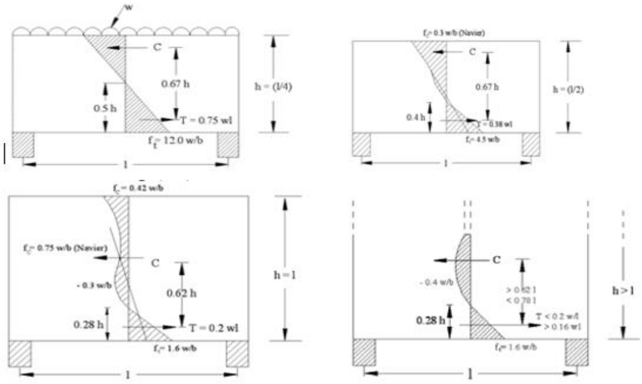

Figure (2) Distribution of Horizontal Flexural Stresses at Mid Span

2. Parametric Study

2.1 Details of Beams for The Analysis

Sixteen RC deep beams are analyzed using finite elements Program (ANSYS 16). The beams are divided to two groups; group 1 for beams which have a compressive strength of concrete (Fcu) 40 MPa, Group 2 for beams which have a compressive strength of concrete (Fcu) 100 MPa. The geometry of the beams is shown in figure (3). The beams have 300 mm wide and effective length 2000 mm. The locations of loads and supports were the same for all beams.

The beams have a different longitudinal reinforcement at the tensile and compression face and different horizontal and vertical reinforcement are shown in figure (4). The longitudinal reinforcement at the top and bottom high strength steel bars with yield stress 360 MPa. The web reinforcement was normal mild steel with yield stress 240 MPa. The details of the reinforced concrete deep beams are summarized in table 1.

The percentage of steel is varied from 0.40 to 2 %. The characteristic compressive strength of concrete is varied from 40MPa to 100MPa. The parametric study on the shear strength of concrete deep beams is carried out using the models proposed by ANSYS software.

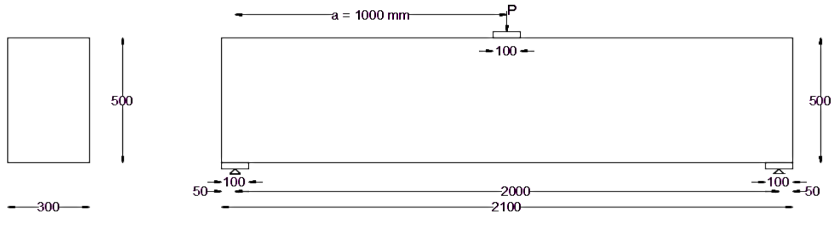

Figure (3) Geometry of the beams

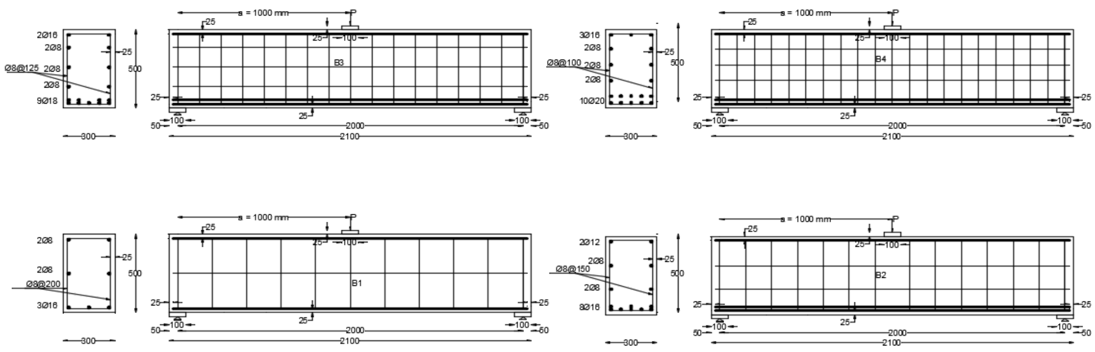

Figure (4) Details of the beams

Table 1 Details of Reinforcement of the Analyzed Beams

Beams ID	Height (mm)	Shear span (a) (mm)	a/d	ρ_L (%)	Bottom RFT.	TOP RFT.	Fy_L (MPa)	HZ.RFT	VL.RFT	Fy (MPa)	F_{cu} (MPa)
Group 1											
B1	500	1000	2	0.40	3φ16	2φ8	360	φ8@200	φ8@200	240	40
B2	500	1000	2	1	8φ16	2φ12	360	φ8@150	φ8@150	240	40
B3	500	1000	2	1.50	9φ18	2φ16	360	φ8@125	φ8@125	240	40
B4	500	1000	2	2	10φ20	3φ16	360	φ8@100	φ8@100	240	40
B5	1000	1000	1	0.40	5φ16	2φ10	360	φ8@200	φ8@200	240	40
B6	1000	1000	1	1	12φ18	4φ12	360	φ8@150	φ8@150	240	40
B7	1000	1000	1	1.5	15φ20	4φ16	360	φ8@125	φ8@125	240	40
B8	1000	1000	1	2	19φ20	5φ16	360	φ8@100	φ8@100	240	40
Group 2											
B9	500	1000	2	0.40	3φ16	2φ8	360	φ8@200	φ8@200	240	100
B10	500	1000	2	1	8φ16	2φ12	360	φ8@150	φ8@150	240	100
B11	500	1000	2	1.50	9φ18	2φ16	360	φ8@125	φ8@125	240	100
B12	500	1000	2	2	10φ20	3φ16	360	φ8@100	φ8@100	240	100
B13	1000	1000	1	0.40	5φ16	2φ10	360	φ8@200	φ8@200	240	100
B14	1000	1000	1	1	12φ18	4φ12	360	φ8@150	φ8@150	240	100
B15	1000	1000	1	1.5	15φ20	4φ16	360	φ8@125	φ8@125	240	100
B16	1000	1000	1	2	19φ20	5φ16	360	φ8@100	φ8@100	240	100

3. Finite Element Modeling

ANSYS [11] is a finite element analysis (FEA) code widely used in the computer-aided engineering (CAE) field. ANSYS[11] software allows engineers to construct computer models of structures, machine components or systems; apply operating loads and other design criteria; and study physical responses, such as stress levels, temperature distributions, pressure, etc. It permits evaluation of a design without having to build and destroy multiple prototypes in testing. The finite elements used in the modeling of the beam link 180, solid 185 and solid 65.

Due to the symmetry in cross-section of the concrete beams and loading, symmetry was utilized in the FEM, only one-quarter of the beam was modeled.

3.1Element types

3.1.1 Concrete

The eight nodes element "SOLID65" is used in the present research to model concrete material. It is used for the 3-D modeling of solids with or without reinforcing bars (rebar). The element is capable of cracking in tension and crushing in compression. The element is defined by eight nodes having three degrees of freedom at each node: translations in the nodal x, y, and z directions, as shown in Figure (5). Up to three different rebar specification may be defined.

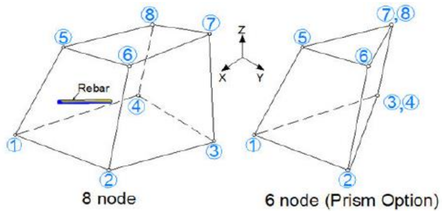

Figure (5) Geometry of the Element SOLID65 [11]

3.1.2 Steel Bars

The one-dimensional two-node element LINK180 is used in the present work to model the rebar. The LINK180 element is a uniaxial tension-compression element with three degrees of freedom at each node: translations in the nodal x, y, and z directions as illustrated in Figure (6). As in a pin-jointed structure, no bending of the element is considered. Plasticity, creep, swelling, stress stiffening, and large deflection capabilities are included. The nodes of this element are aligned with the nodes of the SOLID 65 elements to allow for merging the nodes together. Hence, a perfect bond between concrete and steel is automatically introduced.

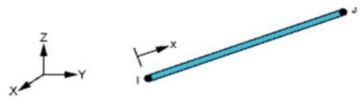

Figure (6) Geometry of the element LINK180

3.1.3 Steel Plates

SOLID185 is used for the 3-D modeling of solid structures. The element is defined by eight nodes having three degrees of freedom at each node: translations in the nodal x, y, and z directions. The element has plasticity, creep, swelling, stress stiffening, large deflection, and large strain capabilities. A reduced integration option with hourglass control is available. SOLID185 elements are used for modeling the support blocks and the load blocks.

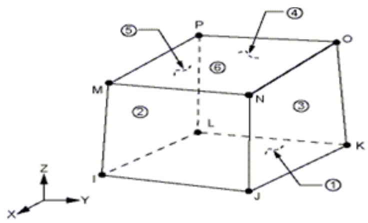

Figure (7) Geometry of the Element SOLID185 [11]

3.2Real Constants

No real constant set for the Solid 185 elements. Concrete ANSYS 16, allows the user to enter three rebar materials in the concrete [11]. Each material corresponds to x, y, and z directions in the element. Real Constant Set 1 is used for the Solid65 element. The other real Constant Sets are defined for the Link180 element. Values for the cross-sectional area were entered. Cross-sectional area in sets 8, 10, 12,16,18,20 refer to the reinforcement of φ 8 stirrups (and HZ.RFT.), φ 10, φ 12, φ 16,φ 18,φ 20 bars respectively. Due to symmetry, set 4 and 9 is half of sets 8 and 18.

3.3Material Modeling

3.3.1 Concrete

Concrete has crushing and cracking possibilities and behaves differently in compression and tension. Figure (8) shows the typical stress-strain curve for normal weight concrete. In compression, the stress-strain curve for concrete is linearly elastic up to about 30 percent of the maximum compressive strength. Above this point, the stress increases gradually up to the maximum compressive strength. After it reaches the maximum compressive strength σcu, the curve descends into a softening region, and eventually, crushing failure occurs at an ultimate strain εcu.

In tension, the stress-strain curve for concrete is approximately linearly elastic up to the maximum tensile strength. After this point, the con cracks and the strength decrease gradually to zero. The modulus of elasticity (E_c), and the modulus of rupture (f_{ctr}) for concrete (which are required in the ANSYS 16 analysis) are both calculated in terms of the concrete compressive strength ($F_{c'}$) as follows:

Ec = 4400$\sqrt{Fcu}$ N/mm2 (1) & f_{ctr} = 0.62$\sqrt{Fcu}$ N/mm2 (2)

The Poisson ratio υ for concrete is usually taken as 0.2

The following equations are used to obtain a simplified stress-strain relationship for concrete

$$f = \frac{Ec * \varepsilon}{\left(1+\left(\frac{\varepsilon}{\varepsilon o}\right)2\right)} \quad \textbf{(3)} \quad \& \quad \varepsilon o = 2Fcu/Ec \quad \textbf{(4)} \quad \& \quad \mathbf{Ec} = f/\varepsilon \quad \textbf{(5)}$$

Where:

f: Stress at any strain & ε: Strain at stress & ε_o: Strain at the ultimate compressive strength

Figure (9) shows this simplified relationship which is used in the present study. Other parameters required to perform the finite element analysis are the shear transfer coefficients. These coefficients range from 0.0 to 1.0, with 0.0 representing a smooth crack (complete loss of shear transfer) and 1.0 representing a rough crack (no loss of shear transfer). This specification may be made for both the closed and open crack. When the element is cracked or crushed, a small amount of stiffness is added to the element for numerical stability.

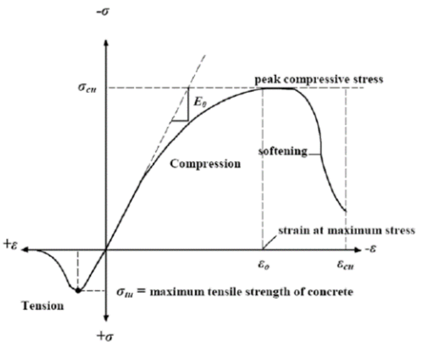

Figure (8) Typical stress-strain curve for concrete

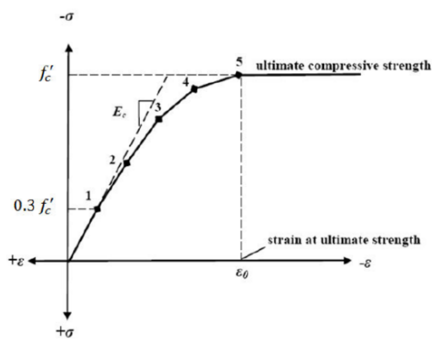

Figure (9) Simplified compressive stress stress-strain curve for concrete

3.3.2 Steel Bars

The bilinear model is used in the present study to represent the stress-strain relationship for steel bars in the ANSYS 16 software.

Table (2) Material models for typical model

Material number	Element type	Material properties					
		Linear Isotropic		**Multilinear Isotropic**		**Non-metal plasticity of concrete**	
		Ex	Acc.to Eq.(1)	stress	strain	Open shear transfer coefficient	0.20
		PRXY	0.20	Acc.to Eq.(3),(4)		closed shear transfer coefficient	0.90
1	Solid 65					Uniaxial cracking stress (f_{ctr})	Acc.to Eq.(2)
						Uniaxial crushing stress (f'_c)	-1
						Biaxial crushing stress	**
						Hydrostatic pressure	**
						Hydrostatic biaxial crush stress	**
						Hydrostatic uniaxial crush stress	**
						Tensile crack factor	**
2	Link 180	**Linear Isotropic**		**Bilinear Isotropic**			
		Ex	200 GPa	Yield stress	360 MPa		
		PRXY	0.30				
3	Link 180	**Linear Isotropic**		**Bilinear Isotropic**			
		Ex	200 GPa	Yield stress	240 MPa		
		PRXY	0.30				
4	Link 185	**Linear Isotropic**					
		Ex	200 GPa				
		PRXY	0.30				

Labeled number ** default input data

3.4Meshing

To obtain good results from the Solid 65 elements, the use of a rectangular mesh is recommended. Therefore, the mesh was set-up such that square or rectangular elements were created. The volume sweep command was used to mesh the steel plate and support. This properly sets the width and length of elements in the plates to be consistent with the elements and nodes in the concrete portions of the model. The overall mesh; of the concrete, steel bars, and support volumes is shown in figure (10). The necessary element divisions are noted. Maximum meshing dimension for all models is 12.5 x 12.5 mm.

3.5Boundary Conditions and loading

Displacement boundary conditions are needed to constrain the model to get a unique solution. To ensure that the model acts the same way as the experimental beam, boundary conditions need to be applied at points of symmetry, and where the supports and loadings exist. The symmetry boundary conditions were set first. The model being used is symmetric about two planes. The boundary conditions for both planes of symmetry are shown in figure (11).

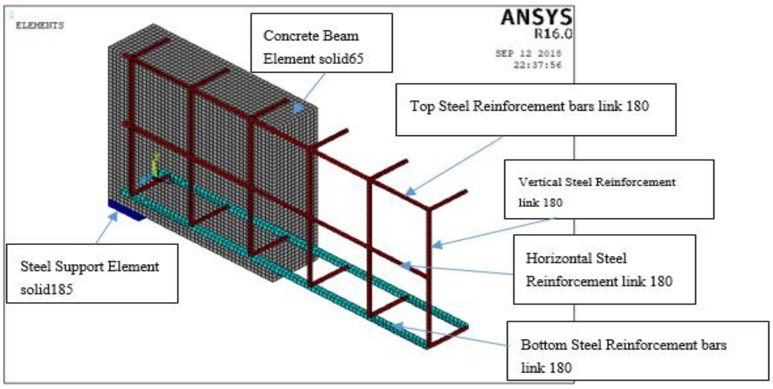

Figure (10) Typical Mesh Configuration in ANSYS for all Beams

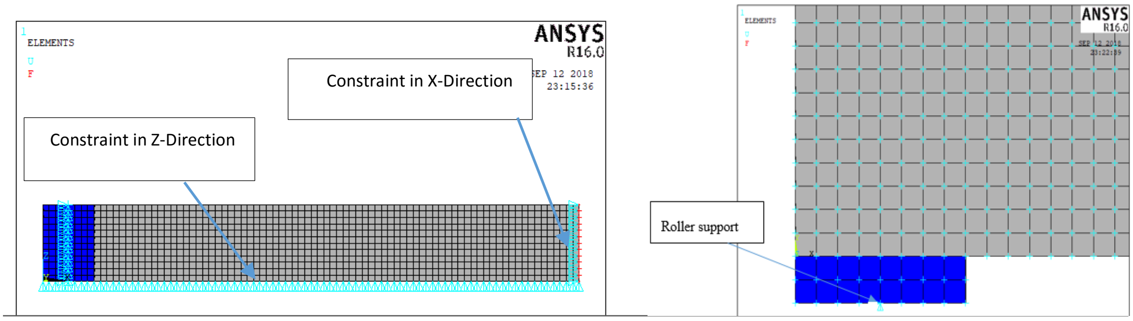

Figure (11)Boundary Conditions for Symmetry and supports in ANSYS for all Beams

Nodes defining a vertical plane through the beam cross-section centroid defines a plane of symmetry. To model the symmetry, nodes on this plane must be constrained in the perpendicular direction. These nodes, therefore, have a degree of freedom constraint UX = 0. Second, all nodes selected at Z = 0 define another plane of symmetry. These nodes were given the constraint UZ = 0. The support was modeled in such a way that roller support was created. A single line of nodes on the plate was given constraint in the UY direction, applied as constant values of 0. The support condition is shown in Figure (11). The static load was applied to cross beam through group of concentrated loads distributed uniformly on steel loading plate nodes as shown in Figure (12)

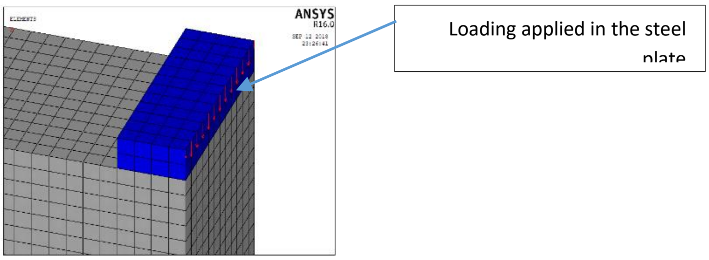

Figure (12) Load application on steel loading plate in ANSYS for all Beams

3.6Non-Linear Solution

In the nonlinear analysis, the total applied load to a finite element model is divided into a series of load increments called load steps. At the completion of each incremental solution, the stiffness matrix of the model is adjusted to reflect nonlinear changes in structural stiffness before proceeding to the next load increment. The ANSYS program uses Newton-Raphson equilibrium iterations for updating the model stiffness [11].

4. Results

The finite element results, including plots of deformational and strain behavior for each model, are presented. To plot the load-deflection and load-strain diagrams, certain points were chosen; these points represent critical locations in the specimens where the maximum values are expected to occur.

4.1Failure Loads and load deflections

Table (3) shows the ultimate load and the maximum deflection at the ultimate load obtained by ANSYS software. The ultimate load obtained by ANSYS software represents the load level at which the concrete reached to its ultimate strain (0.003) for Fcu 40 MPa and (0.0045) for Fcu 100 MPa or the reinforcement reached to the maximum stress which is smaller.

Table (3) Failure load and mid-span deflection for beams at different concrete strength

Beam Number	At Failure Load	
	Failure Load P_u(KN)	Maximum Deflection Δ_u(mm)
Group 1		
B1	310	10
B2	690.48	623
B3	839.52	4.4
B4	1180	6.5
B5	942	1.96
B6	1580	2.91
B7	1862.48	2.82
B8	2232.56	2.85
Group 2		
B9	336	8.25
B10	708.48	2.92
B11	917.16	6.32
B12	1257. 52	3.95
B13	974.48	1.78
B14	2604.48	4.07
B15	3540	3.81
B16	3940	3.86

Figures (13) and (14) show the vertical deflection contour lines for all beams at the failure load when the strain of the concrete reached the maximum value.

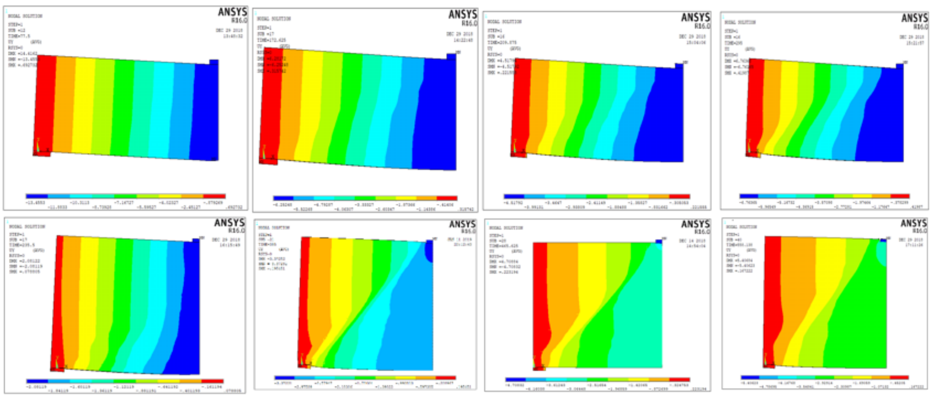

Figure (13) Typical contour lines for deformation at failure extracted from ANSYS model of beams in group 1 from (B1) to (B8) respectively

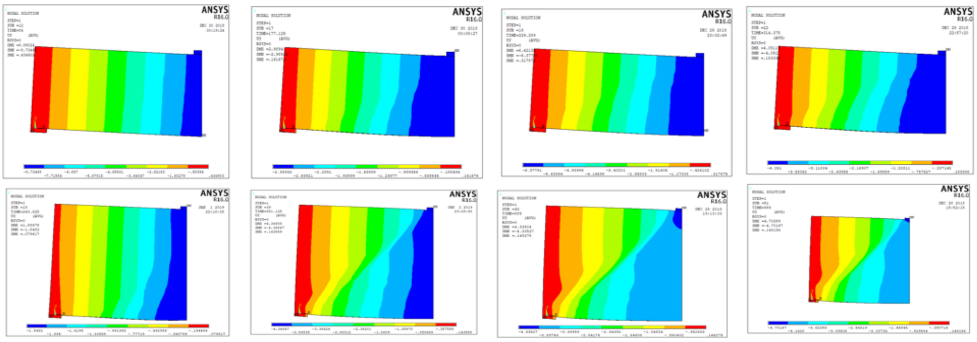

Figure (14) Typical contour lines for deformation at failure extracted from ANSYS model of beams in group 2 from (B9) to (B16) respectively

The measured load-deflection curves for all beams are shown in figure (15). It can be seen from the figure (15) and table 3 that the decrease of shear span to depth ratio (a/t) leads an increase in the load carrying capacity and stiffness at different levels.it can also be seen that all beams which have the same compressive strength of concrete and the same depth have nearly the same value of the first cracking load as the behavior of the concrete depends on the rapture modulus until the first cracking.

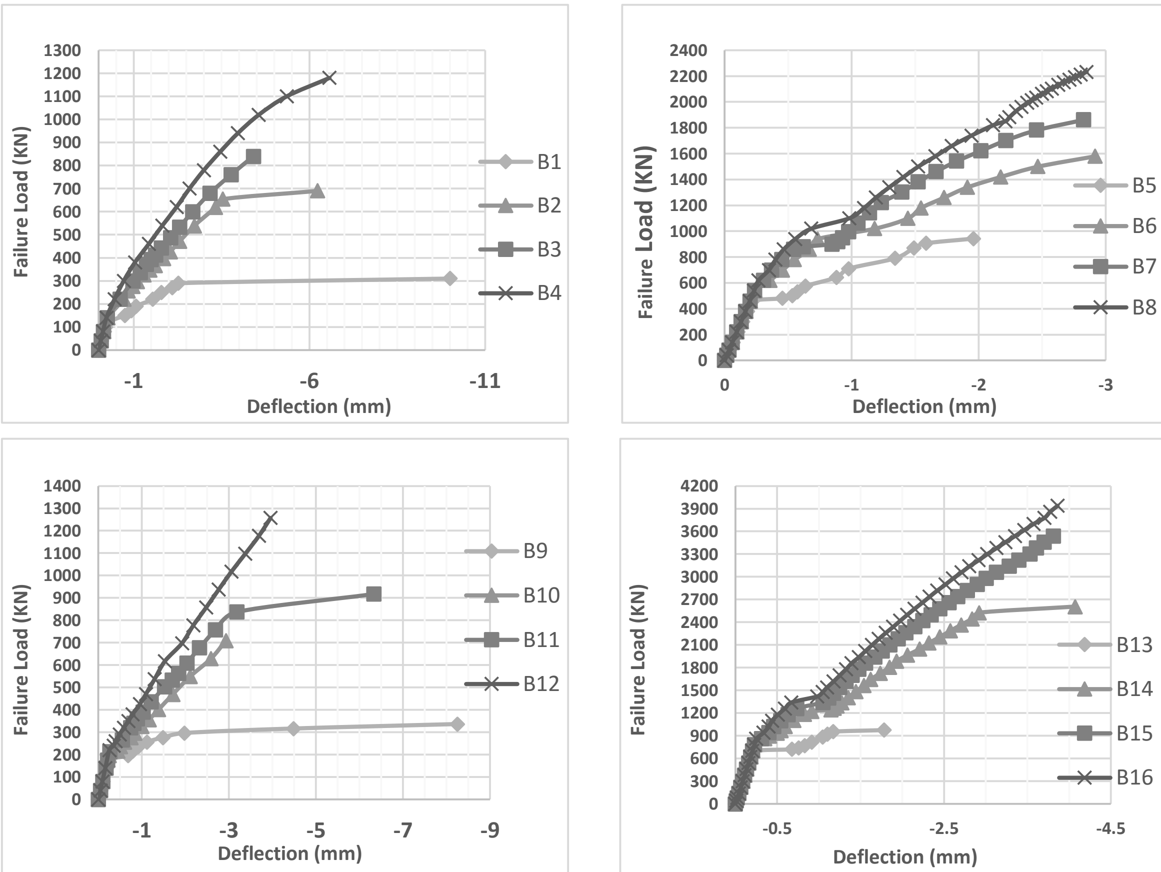

Figure (15) failure load and mid-span deflection relationship for all beams

As seen in figures (15), and table (3) the failure load at moderate strength grade of concrete F_{cu} 40 MPa increase by increasing the longitudinal reinforcement percent as increasing ρ_t from 0.40% for B1 to 2% for B4 resulted in an increase in failure load by about 380.6%. Furthermore, the increasing ρ_t from 0.40% for B1 to 1% for B2 resulted in an increase in shear strength by about 222.7%.Increasing ρ_t from 0.40% as in B5 to 2% as in B8 resulted in an increase in failure load by about 67.8%,97.7%,and 237% respectively .

The failure load at very high strength grade of concrete F_{cu} 100 MPa increase by increasing the longitudinal reinforcement percent as increasing ρ_t from 0.40% for B9 to 2% for B12 resulted in an increase in failure load by about 210.90%,272.9%, and 374.3% respectively. Increasing ρ_t from 0.40% for B13 to 2% for B16 resulted in increase in failure load by about 267.3%, 363.3, and 404.3% respectively.

4.2crack propagation

The following figures show the crack propagation at failure load for the analytical beams using the quarter model in ANSYS program software. In ANSYS [11] program displays circles at locations of cracking or crushing in concrete elements. Cracking is shown with a circle outline in the plane of the crack appears when principal tensile stress exceeds the ultimate tensile strength of concrete, and crushing is shown with an octahedron outline. The first crack at the integration point is shown with a red circle outline, the second crack with a green outline, and the third crack with a blue outline. From the figures below for the beams have the same ratio of reinforcement and different concrete strength; increasing in the compressive strength leads to increasing in failure loads and increasing the cracks propagation. Beams with larger (a/t) showed earlier development of flexural cracks and less well-defined shear cracks. As shown in the figures of the crushing that the failure of deep beams was mainly due to diagonal cracking and it was along the lines joining the loading points and supports (compression strut).

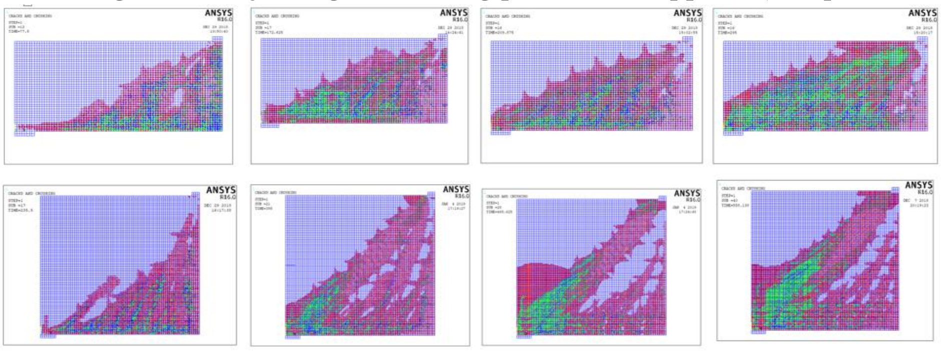

Figure (16) Crack pattern for beams in group 1 from (B1) to (B8) respectively

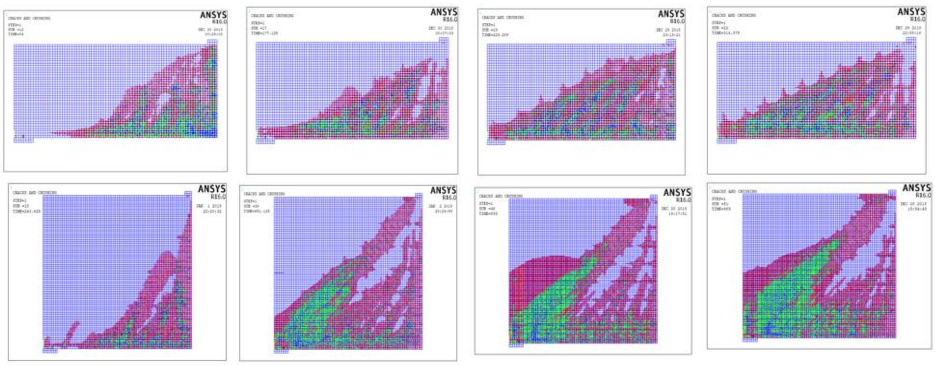

Figure (17) Crack pattern for beams in group 2 from (B9) to (B16) respectively

4.3 Influence of grade of concrete, depth, and ρt on the shear strength of beams predicted using ANSYS 16.0 software

Figure (18) and (19) illustrate the effect of the compressive strength of the concrete and depth on the shear strength of the beams. Changing compressive strength of concrete from 40 MPa to 100 MPa as in beams in group 1 to beams in group 2 respectively resulted in increase in failure load by about 8.4%,2.6%,9.25%,6.6%,3.44%,64.8%,90%,76.5%, and 28.60% respectively; which indicate that the changing Fcu have low effect for beams which have high shear span to depth ratio(a/t=2), otherwise the beams which have small shear span to depth ratio (a/t=1).

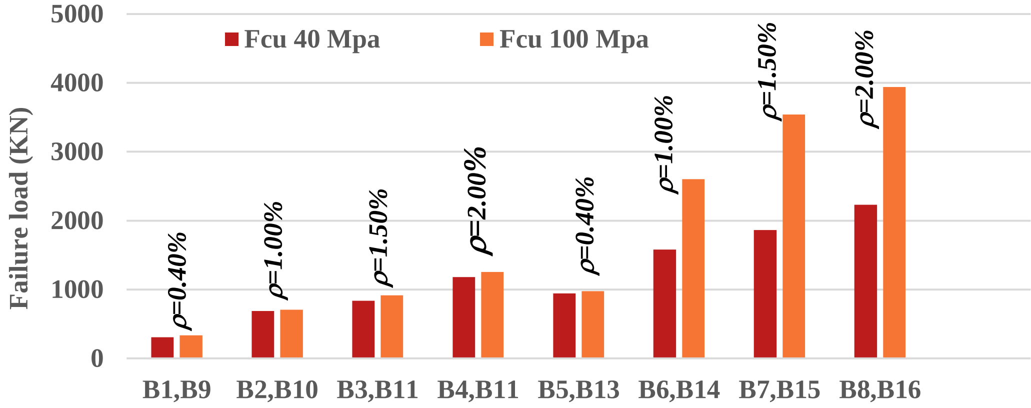

Figure (18) Influence of grade of concrete on shear strength

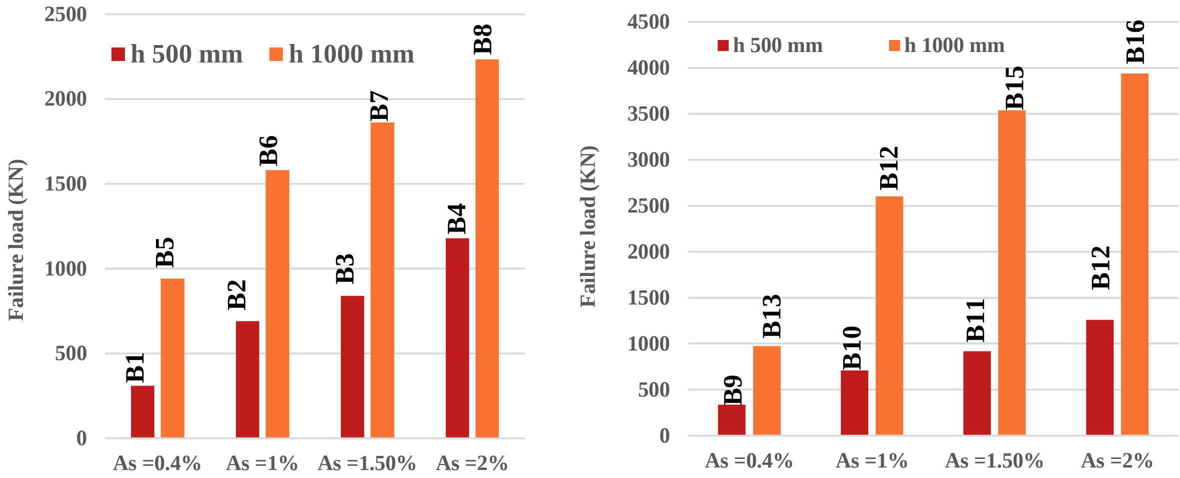

Figure (19) Influence of depth on shear strength

Increasing depth from 500mm to 1000 as in beams B1 and B5 which have the same value Fcu 40 MPa and the same As% 0.40 resulted in increase in failure load by about 303.90%. Increasing depth from 500mm to 1000 as in beams B9 and B13 which have the same value Fcu 100 MPa and the same As% 0.40 resulted in increase in failure load by about 290%. Increasing depth is more effective in increasing the failure load rather than increasing compressive strength.

4.4Steel strain

Figure (20) shows respectively the load steel strain curves for bottom longitudinal flexural reinforcement of all beams at Fcu 40 MPa and Fcu 100 MPa.These figures also indicate that all beams show almost the same total applied load strain gradient with the major strains redistribution in the bottom steel after the first cracking. For beams in group 1 which have higher (a/t) =2, the bottom reinforcement reached to its yielding strain 0.0018 before crushing of concrete reached 0.003 due to the section was under reinforced. Otherwise, the beams which have a lower ratio of (a/t) =1 and have As% from 1% to 2, the strain in the concrete reached to its maximum value 0.003 before the reinforcement reached to the yielding stress due to stress redistribution (compression failure) because the sections were over reinforced. For beams in group 2, all reinforcement in all beams reached to its yielding strain before crushing as the sections were under reinforced (ductile failure).

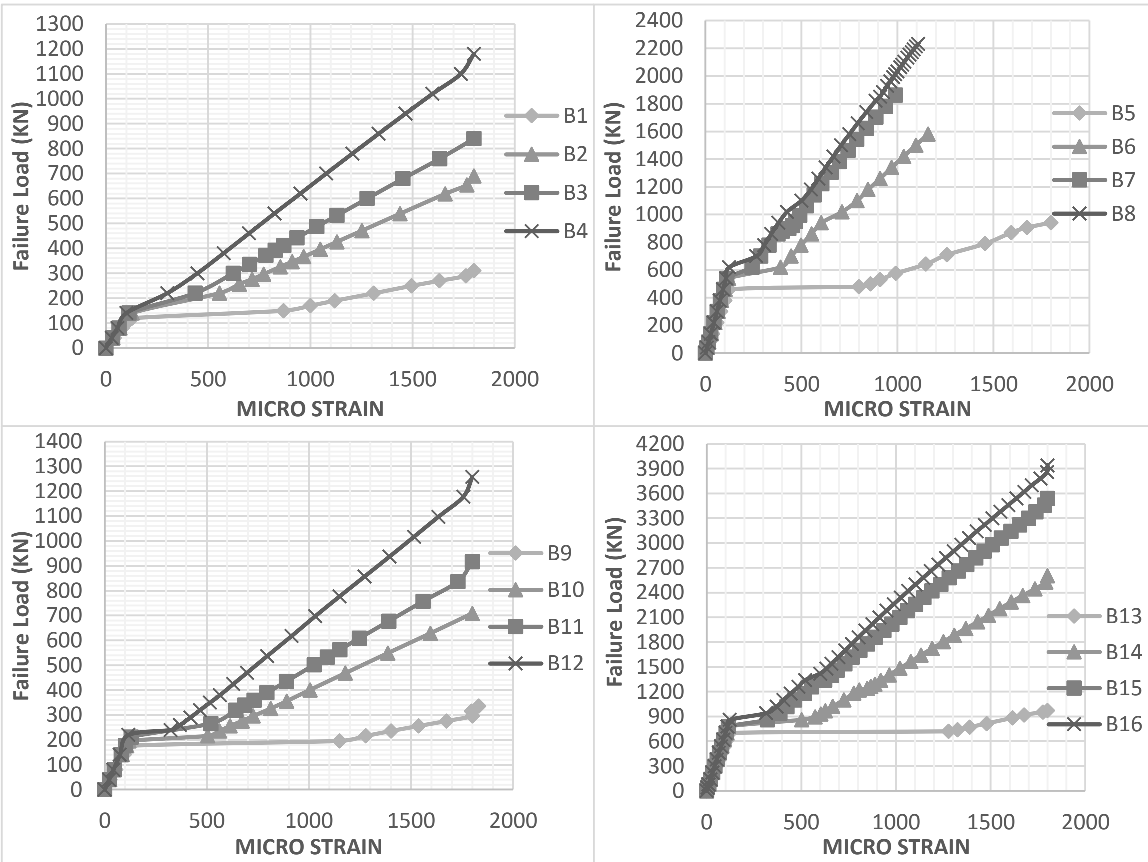

Figure (20) Bottom steel strain for all beams

5. Conclusion

From the analytical studies in the present paper, the following conclusion are drawn:

1. The prediction of load-deflection response, as well as the cracking patterns using the nonlinear finite element program ANSYS 16, show a very well agreement with the testing results from the literature
2. Failure of deep beams was mainly due to diagonal cracking and it was along the lines joining the loading points and supports.
3. It was observed that the smaller (L/d) ratio, the higher the shear strength value.

4. Changing compressive strength of concrete from 40 MPa to 100 MPa has a low effect on the failure load for beams which have high ratio of shear span to depth (a/t=2). Otherwise, the beams which have a small ratio of shear span to the depth (a/t=1) with a high ratio of Reinforcement higher than or equal 1%, the failure load increased nearly twice.

6. References

1. Egyptian Code of Practice, 2010, Design and construction of reinforced concrete, Ministry of building construction, Structural Engineering, Cairo, Egypt.
2. ACI Committee 318, 2008, Building code requirements for structural concrete (ACI 318-08) and Commentary (ACI 318-R-08), American Concrete Institute, Structural Engineering.
3. Indian standard (IS 456: 2000) Code for reinforced concrete code design guidelines
4. Japanese Standard specification for concrete structures (JSCE 2007), Japan society of civil engineering, 34-57 (in japan).
5. Candian Standard Association (CSA 2004), Design of concrete structures code
6. British standard (BS 8810) for the Design and Construction of Reinforced and Prestressed Concrete Structures.
7. Zsutyy, T.C (1968), "Beam shear strength prediction by analysis of existing data", ACI journal proceedings, 65(11), 943-951
8. Mau, T. and Hsu, T.C.(1989), "Formula for the shear strength of deep beams". ACI structural journal, 86(5), pp 516-523
9. Matamoros, A.B. and Wong, K.H. (2000), " Design of simply supported deep beams using strut-and-tie model", ACI structural journal, 100(6), pp 704-712
10. Park, J.W., and Kuchma, D. (2007), "Strut and Tie model analysis for strength predictions of deep beams'. ACI Structural Journal, 104(6), 657-666
11. ANSYS, (2016), Release 16.0 Documentation. ANSYS Inc., http://www.ansys.com.
12. William K.J. and wrank E.P. 1975 Constitutive model for the triaxial behavior of concrete. Proceedings of the International Association for Bridges and Structural Engineering, ISMES, Bergamo Italy.vol.19.
13. Mahmoud Abdou Mahmoud Hassanean et al." Behavior of High Performance Continuous R.C. Deep Beams with Openings and its strengthening". Journal of Engineering Sciences, Vol. 42, No.5, 2014 PP. 1138 – 1162